We are IntechOpen,
the world's leading publisher of
Open Access books
Built by scientists, for scientists

6,900
Open access books available

186,000
International authors and editors

200M
Downloads

154
Countries delivered to

Our authors are among the

TOP 1%
most cited scientists

12.2%
Contributors from top 500 universities

CLARIVATE ANALYTICS
BOOK CITATION INDEX
INDEXED

WEB OF SCIENCE™

Selection of our books indexed in the Book Citation Index
in Web of Science™ Core Collection (BKCI)

Interested in publishing with us?
Contact book.department@intechopen.com

Beyond a Nature-inspired Lotus Surface: Simple Fabrication Approach Part I. Superhydrophobic and Transparent Biomimetic Glass Part II. Superamphiphobic Web of Nanofibers

Hyuneui Lim

Department of Nature Inspired Mechanical Systems, Nano Convergence and Manufacturing Systems Research Division, Korea Institute of Machinery and Materials, 171 Jang-dong, Yuseong-gu, Daejeon, 305-343 Korea

1. Introduction

Nowadays, many people have a dream of mimicking the amazing aspects of nature, in particular their functional surfaces. In nature, there are a great many wonderful functional surfaces, such as the lotus leaf for self-cleaning, a morpho-butterfly wing for structural color, a moth eye for antireflection, the back of a stenocara beetle to capture fog, the foot of a gecko for dry adhesion, a strider's leg for water resistance, or a snake's skin as a low friction material [1]. Because biological systems change depending on the environment and circumstances, the surfaces which are always exposed to the outside are well developed for their function, especially in an optimized state. The most interesting feature is that the functional surfaces in nature have a hierarchical structure ranging from macrosize to nanosize as well as a chemical composition that facilitates low surface tension to maximize their role.

Among the numerous nature surfaces, this paper focuses on the lotus leaf, a well-known example of a superhydrophobic and self-cleaning surface [2-4]. The lotus is a plant that can grow in murky ponds. The lotus leaf is a symbol of purity in the Orient, because their leaves always remain clean and dry. This phenomenon originated from the non-wetting property of the lotus leaf. The lotus leaf has two levels of roughness structures comprised of both micrometer-scale bumps and nanometer-scale hair-like structures on the surface with a composition of wax. The trapped air on the rough surface makes water droplets bead up at a contact angle in the superhydrophobic range of 150º and then rolls off while collecting any compiled dirt due to the very low sliding angle.

In order to prove the transfer of this lotus effect to be technically feasible, there have been numerous attempts to synthesize the surface structures on the low surface tension chemical layer. Fabrication methods have been developed to create structures that mimic the superhydrophobic behavior of lotus surfaces, and these are generally categorized into one of two methods: a top-down or a bottom-up method. The top-down processes can structure

patterns well according to the design for superhydrophobicity. Photolithography is one of the most important methods among the top-down processes.[5] capillary lithography [6], electron beam lithography [7], interference lithography [8], pattern transfers of natural surfaces, plasma etching without a mask [9], laser ablation [10], and electrospinning [11] are all top-down processes. The bottom-up processes include colloidal assembly [12], the sol-gel method [13], and the plasma-enhanced chemical vapor deposition of carbon nanotubes. In addition, a combination of bottom-up and top-down approaches [14,15] has been shown to be very useful when fabricating fractal microstructures and nanostructures with superhydrophobic properties.

However, the important aspect of a practical application of superhydrophobic surfaces in daily life is the durability and stability of superhydrophobic micro/nanostructures and the economic feasibility of the fabrication process. Recently, many researchers who study superhydrophobic surfaces have turned their research focus to the durability and stability of superhydrophobic micro/nanostructures and simple fabrication methods for mass production [16-17].

Another issue associated with a superhydrophobic surface is to creation of an amphiphobic surface which repels both water and organic liquids. The demand an oil-repellent surface has increased in many applications, including cell phones and touch-screen displays as well as biomedical devices. Unfortunately, an oil-repellent surface in nature has yet to be reported. Beyond the superhydrophobic lotus surface, researchers have formulated several important considerations with regard to the design of an amphiphobic surface [18,19].

In this review paper, superhydrophobic and transparent biomimetic glass and a superamphiphobic web of nanofibers are introduced. The fabrication method, advantages of biomimic surfaces, and their limitations in practical applications are discussed to help the understanding on the advance of the lotus effect. The results are mainly based on two published articles: "Simple Nanofabrication of a Superhydrophobic & Transparent Biomimetic Surface" in Chinese Science Bulletin [20], and "Superamphiphobic Web of PTFEMA Fibers via Simple Electrospinning without Functionalization" in Macromolecular Materials and Engineering [21].

2. Superhydrophobic and superhydrophilic plant leaves in nature

It is very well known that the lotus leaf, which shows a superhydrophobic property, has a dual roughness characteristic based on the microscale and nanoscale dimensions. Including the lotus leaf, there are many plants that have the ability to repel water in nature. Commonly, they have hierarchical structures on their surface. However, some plant leaves have the ability of superhydrophilicity, in which the water contact angle is less than 10°. Their surfaces can either spread water widely over a wet surface or absorb water via porous structures.

Figure 1 shows an image of superhydrophobic and superhydrophilic plant leaves. The lotus leaf and the taro leaf show a similar surface morphology with nano patterns on micro conical structures with a diameter of around 10μm, representing the superhydrophobic structure. However, the water lily shows only a microstructure having superhydrophilicity without nanoscale structures. This is very interesting because both the water lily and the lotus are aquatic plants. However, the water lily leaves are positioned on the water's surface, whereas the lotus leaves elevate several feet above it. Therefore, their surfaces are adapted to an ambient environment very intelligently.
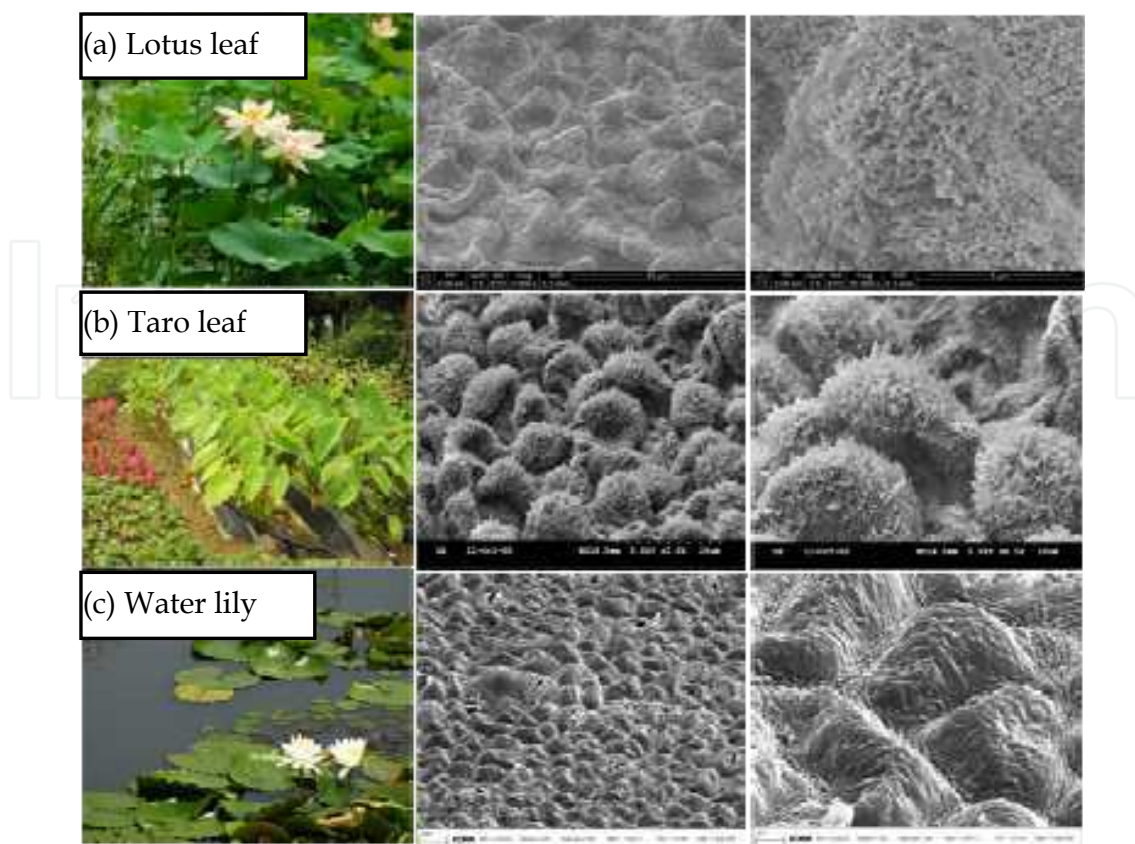
Fig. 1. Optical and SEM images of plant leaves showing the superhydrophobic and
superhydrophilic characteristics: (a) lotus leaf, (b) taro leaf, and (c) water lily

Part I. Superhydrophobic and transparent biomimetic glass

A combination of colloidal lithography and plasma etching is a good candidate to create
well-ordered micro/nanostructured surfaces easily. In particular, superhydrophobic and
transparent glass can be created using only nanobeads smaller than 100 nm to maintain the
proper level of transparency [22]. Here, a combination of colloidal lithography and plasma
etching is used to fabricate superhydrophobic and transparent glass.

A schematic diagram of the fabrication process is shown in Figure 2. First, quartz glass is
prepared after cleaning it by immersion in an Alconox solution (Sigma, Inc.). A water drop
deposited on the cleaned dry glass surface shows a contact angle of nearly 0° without any
particles of dust. Single layers of polystyrene beads were formed by spin coating as a
colloidal mask. Polystyrene beads (Polysciences, Inc.) with diameters of 100 nm (S.D. = 4%)
were purchased in the form of an aqueous suspension. The polystyrene bead solution was
diluted to 0.6% with a mixture of methanol and triton X-100 to increase its volatility and to
prevent aggregation. Spin-coating of the polystyrene nanosphere solution was performed at
different spin rates for 1 minute and the quartz glass was then etched with a mixture of CF_4
and H_2 gas to enhance the etching selectivity. Finally, chemical coating of the low-surface-
tension composition was done to obtain the superhydrophobic property. Additional
information concerning this experimental method is available in the literature [20].

Figure 3 shows SEM images the spin-coated polystyrene beads created under several
conditions, in the case 1000 rpm, 2000 rpm, 3000 rpm, 4000 rpm, and 5000 rpm, for each
sample. The polystyrene beads do not spread well at a low spin rate i.e., 1000 rpm; whereas

the beads are better dispersed at a relatively high spin rate i.e., 4000 and 5000 rpm. The coverage of the nanospheres derives from the balance between the spin rate and the volatility and viscosity of the colloidal suspension in the shear alignment process [23]. Among several spin rates, 3000 rpm resulted in the best spin-coated polystyrene bead layer.
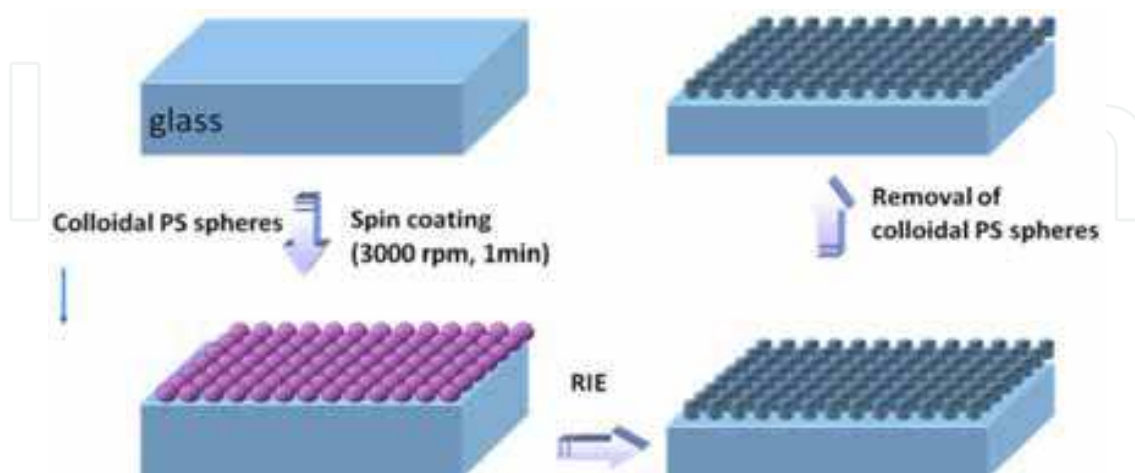

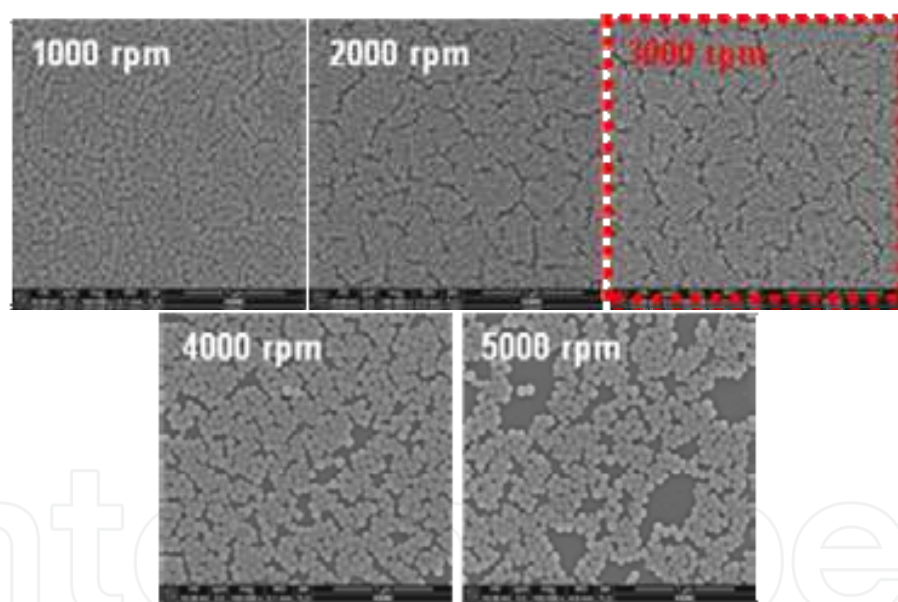Fig. 2. Schematic diagram of the fabrication method

Fig. 3. SEM images of polystyrene bead layers spin-coated at different spin rates: 1000, 2000, 3000, 4000, and 5000 rpm

SEM images of polystyrene beads that were spin-coated well are shown in Figure 4. They have a single layer with close-packed and hexagonally ordered shapes. The polystyrene bead layers were also formed without defects or multiple polystyrene bead layers at an optimum spin rate, i.e., 3000 rpm.

However, for the etching process of the glass, the space between the beads of the colloidal mask requires for a reactive ion treatment on the glass surface. Therefore, spin-coated polystyrene beads were etched with CF_4 plasma for 30 seconds at a RF plasma power of 100 W to decrease the diameters of the beads. Figure 5 shows SEM images of the formed spacing

between the colloidal mask beads. An interparticle distances between the beads of around 20 nm was chosen for the glass etching space.
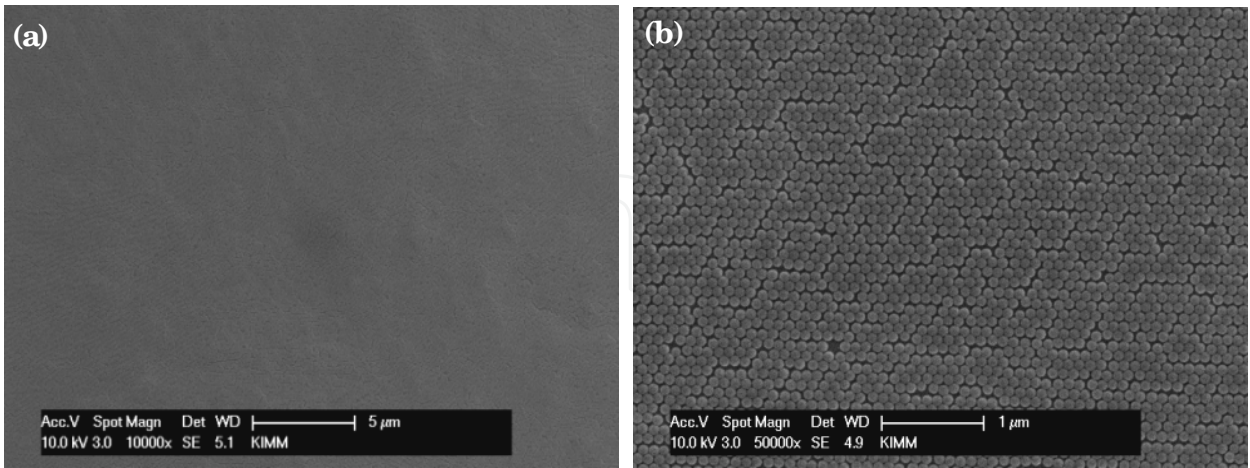

Fig. 4. SEM images of a single layer of polystyrene beads with diameters of 100 nm prepared by spin-coating at 3000 rpm: (a) an image at 10000X magnification, and (b) an image of 50000X magnification [20]
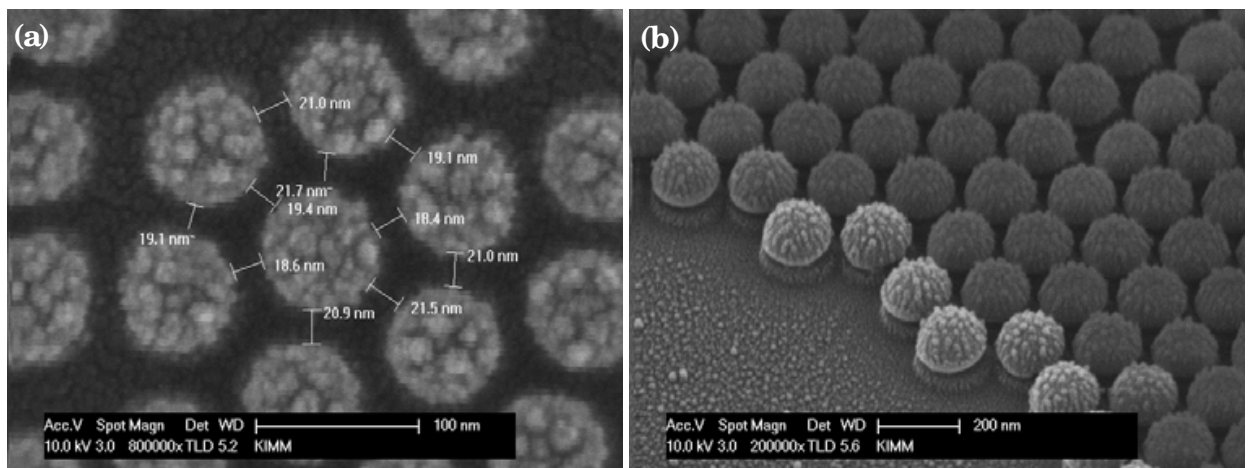

Fig. 5. SEM images of a reactive ion etching (RIE)-assisted colloidal mask of single-layered polystyrene beads treated with CF_4 plasma for 30 s; (a) top-view and (b) tilted view at 30° [20]

The nanostructures on the glass surface were formed by etching with the modified colloidal mask. Generally, glass surfaces are etched with CF_4 or SF_6 plasma. However, the use of only CF_4 plasma can lead to etching of the glass surface as well as over-etching of the 100 nm polystyrene beads, as shown in Figure 6(a). To formulate a nanostructure with a high aspect ratio, conservation of the polystyrene beads is critical during the etching process. The addition of H_2 plasma can serve as a solution and thus can protect the polystyrene beads. Figure 6(b) shows the result of the selective etching of the glass surfaces with a mixture of CF_4 plasma and H_2 plasma at a ratio of 2:1. Depending on the portion of the H_2 plasma, the selectivity between the polystyrene colloidal mask and the glass changed. When a greater amount of H_2 plasma was added, the selectivity of the etching was increased. On the other hand, the etch rate of the glass was reduced.
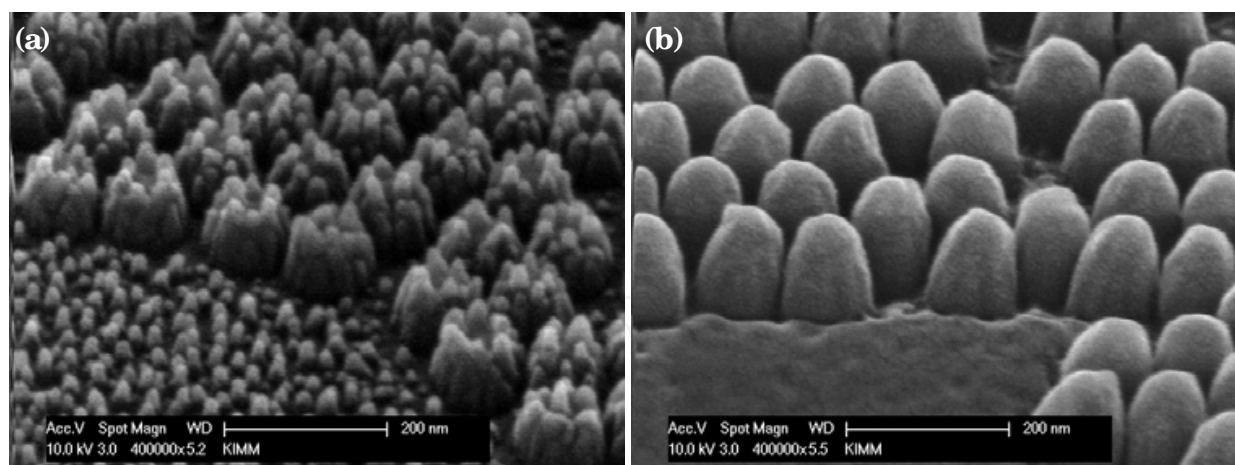
Fig. 6. SEM images of a nanostructured glass surface etched with (a) CF_4 plasma and (b) a mixture of CF_4 plasma and H_2 plasma at a ratio of 2:1 for 3 min. The SEM images were obtained at a tilted view of 30°.

Figure 7 shows the nanostructured glass surfaces according to the etching time with a mixture of CF_4 plasma and H_2 plasma at a ratio of 2:1. The heights of the nanostructures are in direct proportional to the etching time. The nanostructures on the glass surface formed a sharp end on the top and reached a height of nearly 500 nm after 11 minutes of etching. The etching rate in the given reactive ion etching condition was approximately 40 nm/min.
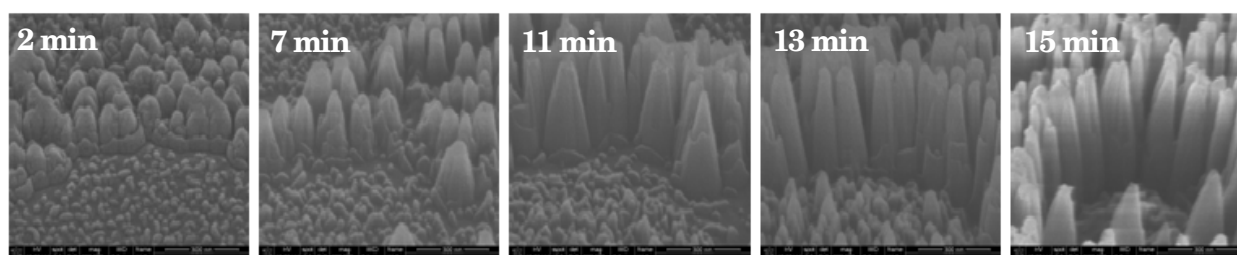

Fig. 7. SEM images of nanostructures on a glass surface etched with different etching times: 2, 7, 11, 13, and 15 min

A high-magnification image of the fabricated nanostructures is shown in Figure 8. This SEM image was obtained under environmental SEM conditions of a low pressure and a low applied voltage of 3 keV without a platinum coating. Compared to the conventional SEM images, the tower-shaped nanostructures have a sharp end on the top. This suggests that the actual shape of the nanostructures is slightly different from that shown in the SEM images when the image is obtained with a metal coating to prevent electron charging on the insulating surface of the sample. The aspect ratio the glass nanostructure was noted to be close to 4 after 10 minutes of etching.

As mention in the introduction, two main factors govern the wettability. The important factor is the chemical property of the surface. When the surface is made up of low surface energy chemicals, a geometrical surface structure enhances the hydrophobicity [24]. The geometrical surface structure of a solid is determined by the fractal structure and the roughness. Therefore, the as-prepared nanostructure glass samples must be modified chemically to obtain surface hydrophobicity.

Self-assembled monolayers (SAMs) of tridecafluoro-1,1,2,2-tetrahydrooctyltrichlorosilane (FOTS) were used as the low surface tension chemical. FOTS SAMs were deposited using a

vapor-deposition method after glass etching and the removal of the remaining polystyrene beads from the top of the nanostructures. An ash process with 30 seconds of O_2 plasma following the CF_4 etching process was applied to remove the remaining polystyrene from the top of the nanostructures. The treated glass samples were then placed in a plastic container with 100 µL of FOTS droplets. Monolayer-assembled deposition was performed for 30 minutes at room temperature. The vapor deposited samples were annealed at 80ºC for 1 hour to stabilize the bonding between the glass surface and the FOTS molecules as well as to increase the well-ordered packing of the FOTS molecules.
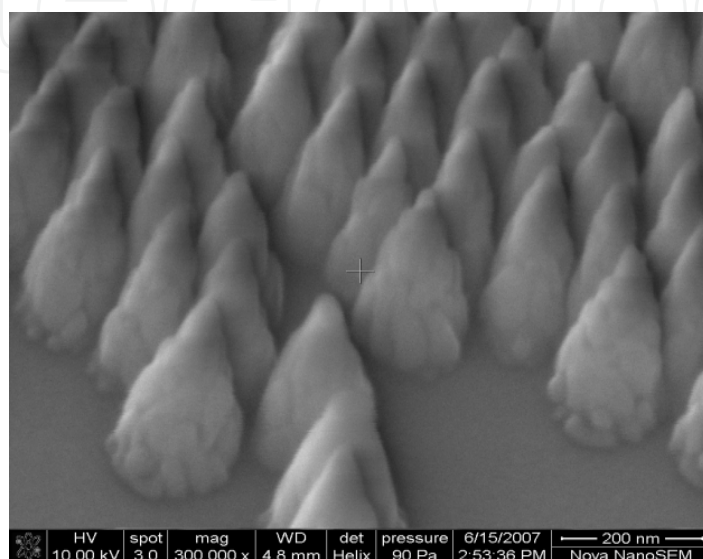

Fig. 8. SEM image of glass nanostructures after plasma etching for 10 min. The image was obtained under environmental SEM conditions without a metal coating.

Figure 9 shows the water contact angles of the nanostructured glass surfaces before and after the low-surface-tension chemical treatment. The wettability of the surfaces was measured with a contact angle analyzer (Phoenix 300, SEO Inc.) with deionized water droplets of 10 µL in volume. The water contact angle of the nanostructured glass surface was close to 4º (Figure 9(a)). The nanostructures on the surface enhanced the hydrophilicity depending on the nature of the flat glass surface. However, the nanostructured surfaces with the FOTS SAMs coating showed superhydrophobicity, with a water contact angle of nearly 150° (Figure 9(b)). Figure 9(c) clearly shows the superhydrophobicity of the fabricated glass. This superhydrophobic glass surface also shows a hexadecane contact angle of 110° given a volume of 10 µL. In the relationship between the superhydrophobic property and the height of the nanostructure, the contact angle of both the water and hexadecane increased steadily as the height of the nanostructure increased to an aspect ratio of 2.5.

In the fabrication of superhydrophobic glass, an important requirement is to retain the transparency of the glass. Therefore, only the use of a nanostructure smaller than the visible wavelength of light can enhance the wettability without leading to opacity. The transmittance of the superhydrophobic glass surface with a nanostructure diameter of 100 nm and different heights in the range of 50 nm to 1000 nm was investigated by UV-Visible spectrometry. Figure 10(a) shows the UV-Visible spectra of the nanostructured glasses with the FOTS SAMs coating and the bare quartz glass as a reference. In the range of the visible wavelength of 400 nm to 700 nm, it was determined that the antireflective phenomena known as the moth-eye antireflection effect existed. A decrease in the transmittance to less

than the 500 nm wavelength was detected in several samples having a relatively high height. This may have originated from the scattering of the light given the high height of the nanostructures. However, the overall transmittance increases due to the decrease in the reflection on the nanostructured glass surface. Finally, a superhydrophobic and antireflective glass having a well-ordered nanostructure was demonstrated, as shown in Figure 10(b).
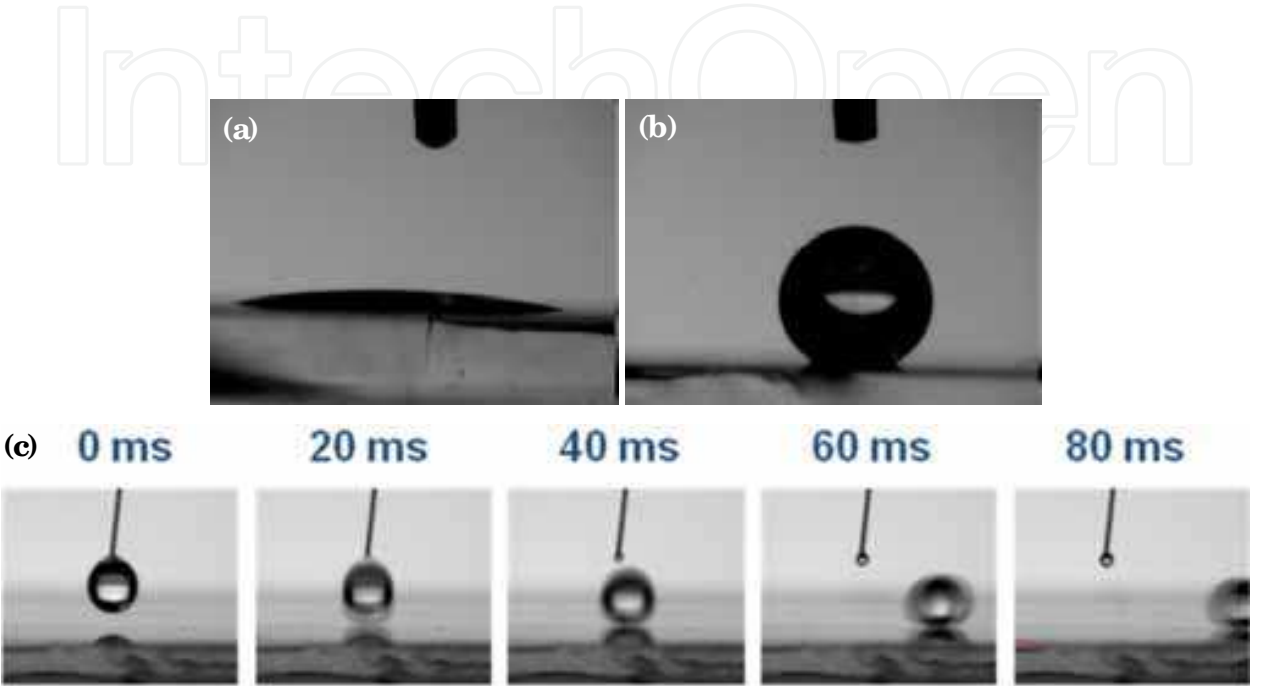

Fig. 9. Images of the water contact angles for (a) a nanostructured glass surface and (b) a nanostructured glass surface after the FOTS SAMs coating. The water contact angles are 4° and 150°, respectively [20]. (c) Sequential images of water droplets falling onto the nanostructured glass surface after the FOTS SAMs coating. The aspect ratio of the nanostructure is 4.
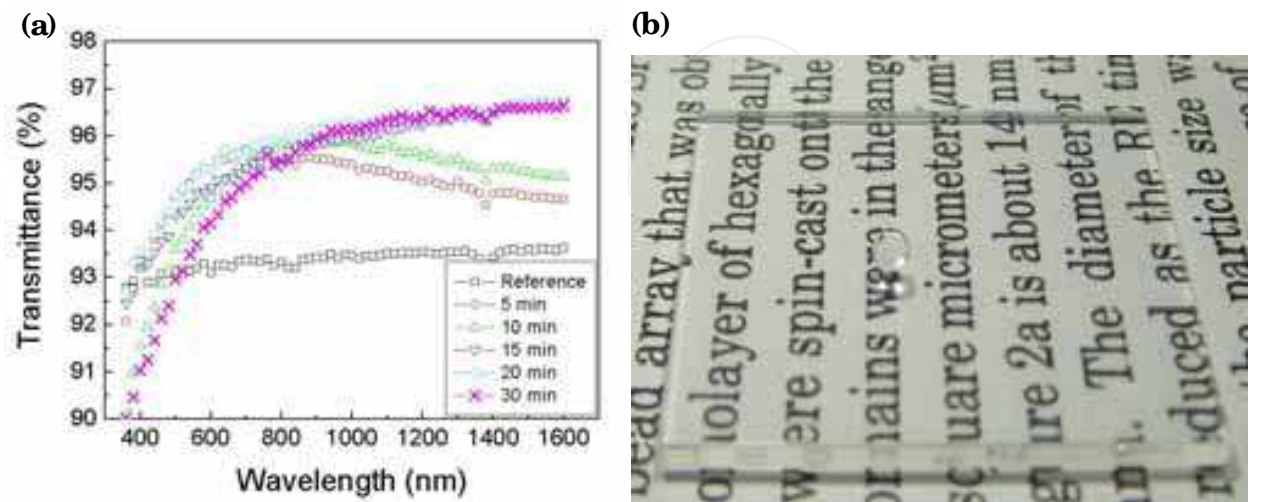

Fig 10. (a) 5 nanostructured and hydrophobic coated glasses with the different etching time and bare sample, and (b) an image of water on the superhydrophobic nanostructured glass [20]

Part II. Superamphiphobic web of Nanofibers

Currently, many researchers are interested in the demonstration of multifunctional surfaces having dual properties such as a superhydrophobicity and antireflective surface, an antifogging and antireflective surface, a switchable surface, a repellent surface capable of repelling several types of liquids, and others. Particularly, surfaces that repel water and organic liquids have recently received a great deal of attention from research and industry fields. Several important findings pertaining to amphiphobic surfaces have been reported with regard to the design of surfaces [18,19].

Two factors should be also considered in the design of a superamphiphobic surface: the chemical composition and structural morphology. For organic liquids, it is impossible to find a chemical layer that yields a contact angle greater than 90° on a flat surface [25,26]. Thus, a structural morphology must be created in which the surface curvature exhibits extreme surface resistance to wetting from all liquids. It is known that the entrapment of air beneath a re-entrant structure prevents the transition from a nonwetted state to a wetted state, even for liquids with low surface tension [27-29].

Of all the re-entrant structures, webs of microfibers and nanofibers are good candidates for a superamphiphobic surface because an electrospinning method can easily produce microfibers and nanofibers from a variety of polymeric materials [30]. In addition, the diameter of the fibers and the gap distance between the electrospun fibers can be controlled according to the processing parameters, such as the solvent, viscosity, surface tension, and electrical conductivity. Therefore, to obtain the information on robustness against wetting from low surface tension liquids, microfibers and nanofibers can form a various superamphiphobic surface. Here, an electrospun web of poly(2,2,2-trifluoroethyl methacrylate) (PTFEMA) fibers is studied to obtain an understanding of a superamphiphobic surface. The morphology of this web is modulated by changing the polymer solution concentration with other fixed processing conditions. That is, we used an applied voltage of 20 kV, a distance of 20 cm between the syringe needle tip and the collector, and a flow rate of 0.2 mL/h. A detailed description of the experimental method was introduced in earlier research, including the synthesis and electrospinning conditions of the PTFEMA as well as the characterization methods of the electrospun nanofibers web [21, 31].

A remarkable feature is that the fabrication of a web of superamphiphobic fibers was performed using a conventional electrospinning process of fluorinated polymers without any additional functionalization. A PTFEMA solution can be electrospun well with conventional processing parameters, as synthesized PTFEMA dissolves homogeneously and easily in several solvents, including Dimethyl foramide (DMF), which is an adequate solvent for electrospinning. To investigate the wetting property of the web, first the surface chemical compositions of the PTFEMA web were analyzed by XPS. An electrospun electrospun and solution casted PTFEMA sample were prepared prepared from a 26 wt% solution of DMF. The fluorine content (F/C ratio) was outstandingly high, at 0.57, and the water contact angle was 153° for the elecrospun sample, whereas the solution casting PTFEMA film showed an F/C ratio of 0.40 and a water contact angle of only 89°. The enrichment of the fluorocarbon composition and the water contact angle of the electrospun PTFEMA were caused by the surface segregation, the high ratio of the surface area to the volume, and by the rough surface morphology [32].

Figure 11 shows the superamphiphobicity of the electrospun nanofiber web. The web of PTFEMA repels both types of liquids shown in the figure, one with a surface tension of 72.8 mN/m (water colored with blue ink) and the other with a surface tension of 27.8 mN/m (hexadecane colored with red ink), while exhibiting contact angles greater than 150°.
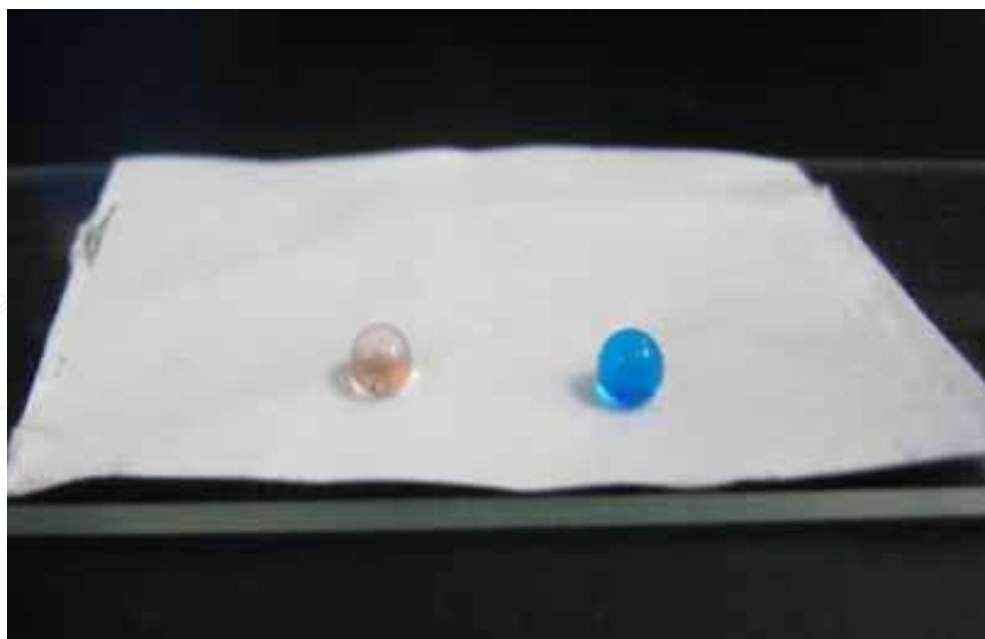
Fig. 11. Photograph of 6 µL droplets of hexadecane (colored with red ink) and 6 µL droplets of water (colored with blue ink) on an electrospun web of PTFEMA fibers with a 26 wt% polymer solution concentration concentration [21]

All of the electrospun webs of PTFEMA fiber are typical superhydrophobic surfaces, showing water contact angles that exceed 150°. However, the wetting response of the low surface tension liquid hexadecane differed depending on the morphology of the fiber webs. The sample prepared from the 26 wt% solution had the thinnest fiber diameter of approximately 500 nm and the narrowest diameter distribution, ranging from 300 nm to 700 nm; its surface repels hexadecane with a high contact angle of around 154°, as shown in Figure 12(a). However, Figure 12(b) shows that the fiber web electrospun with a 24 wt% concentration is different in terms of the fiber diameter and hexadecane contact angle. The 24 wt% sample had an average diameter of 600 nm and considerable variation in its fiber diameters, with some very thick fiber diameters of around 2000 nm or 3000 nm. In addition, the hexadecane droplet collapses with a contact angle of approximately 25° despite the fact that its surface exhibits superhydrophobicity.

The interaction between hexadecane and a web of PTFEMA fiber was investigated to confirm the wetting property of the 24 wt% samples. We obtained SEM images to determine how the morphology of the web changes after soaking the fiber web with hexadecane. As shown in Figure 13, an appreciable change was not detected after the soaking test, which proves that PTFEMA does not react with or dissolve in hexadecane.

The robustness parameter was studied to elucidate the wetting and nonwetting phenomena of hexadecane on superhydrophobic nanofiber webs with different fiber diameters. We used the robustness equation developed by Tuteja and Choi to reveal the relationships among the robustness, the fiber diameter, and the degree of porosity [19]. A detailed explanation of the robustness of fiber web samples is available in the literature [21]. The calculated robustness shows how the hexadecane droplet is sustained on the 26 wt% sample and why it collapses on the 24 wt% sample.

Figure 14 shows a summary of the hexadecane robustness and contact angle in relation to the gap distance and fiber radius depending the PTFEMA solution concentration. When the

apparent contact area is identical, a thinner fiber and lower porosity increase the robustness. The 24 wt% sample shows low robustness, explaining why the hexadecane droplet collapsed although it had a high water contact angle. The 26 wt% sample had the highest level of robustness, keeping the hexadecane droplet intact for more than 8 hours. Figure 14 suggests that the 28 wt% sample and the 30 wt% sample repel the hexadecane droplet for quite a long time. The assumption that the diameter and gap distance of the fibers on the nanofiber surface are homogeneous in terms of the robustness equation implies that the 24 wt% sample has a relatively high level of robustness. However, local variation in both the fiber diameter and the distribution in our samples caused local weak spots to arise with a
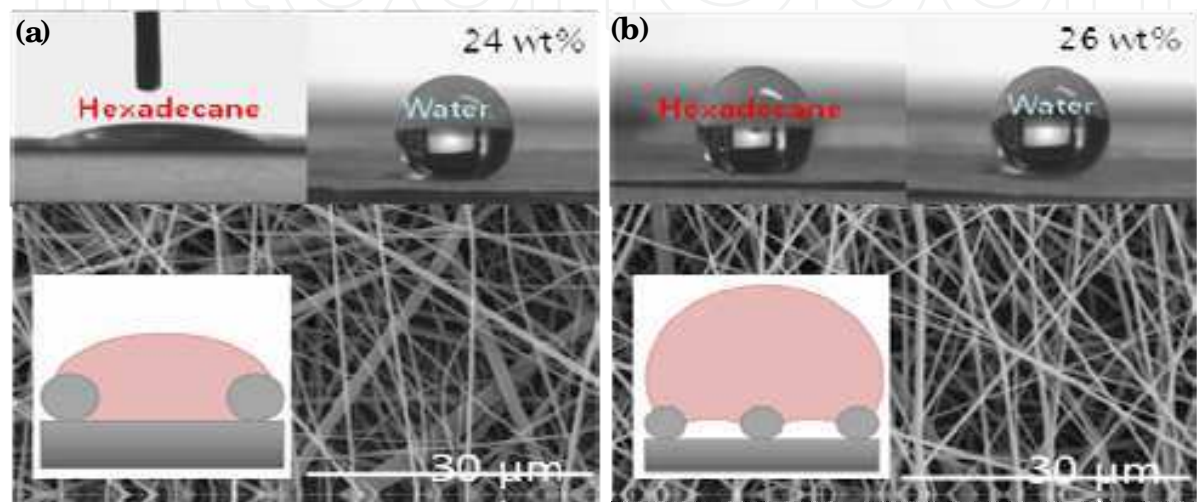
Fig. 12. Hexadecane and water contact angle images, SEM images, and schematic diagram of a nanofiber web with a hexadecane droplet. PTFEMA fibers were electrospun with different polymer solution concentrations: (a) 24 wt% and (b) 26 wt%. The volume of both the hexadecane and the water was 6 μL [21].
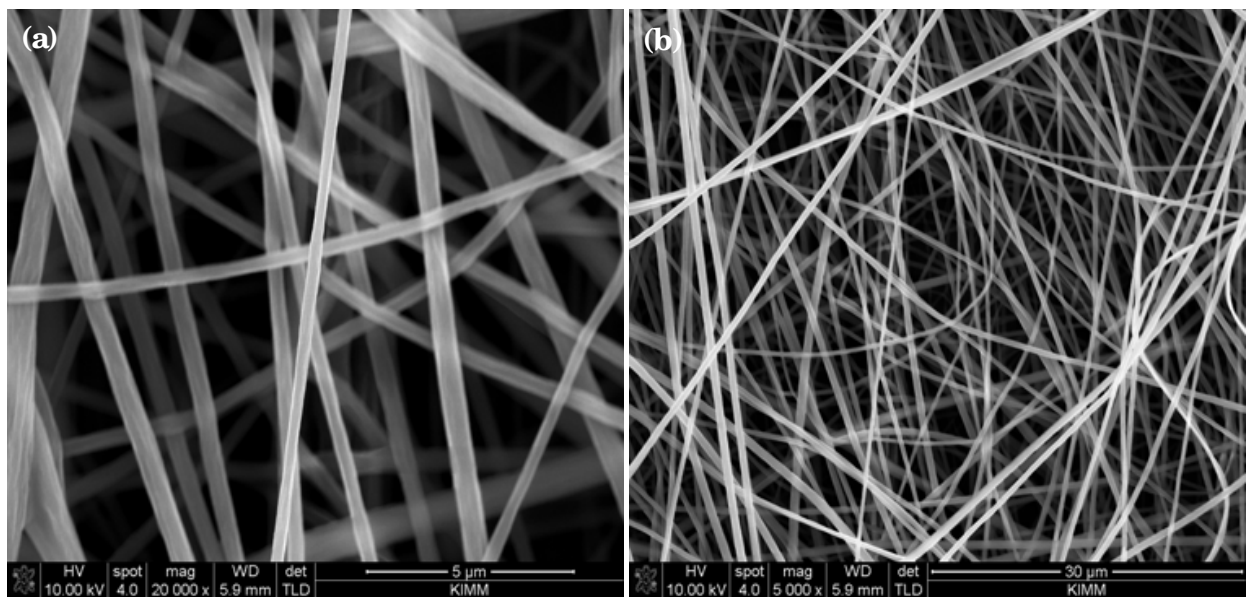

Fig. 13. SEM images of PTFEMA fibers electrospun from 24 wt% after soaking with hexadecane: (a) 5000X magnification, and (b) 20000X magnification

low level of robustness, and the droplet consequently collapsed in those areas. This lower local robustness of the 24 wt% sample can govern the collapse of the hexadecane droplet.

From these results, that control of the wettability against high and low surface tension liquids can be attained by modulating the morphology of the surface, even though the chemical composition is identical. Therefore the fiber diameter and the porosity should be carefully designed to yield a high contact angle and a high level of robustness, as the porosity is related to the contact angle: that is, a high porosity value yields a low contact area and, consequently, a high contact angle.
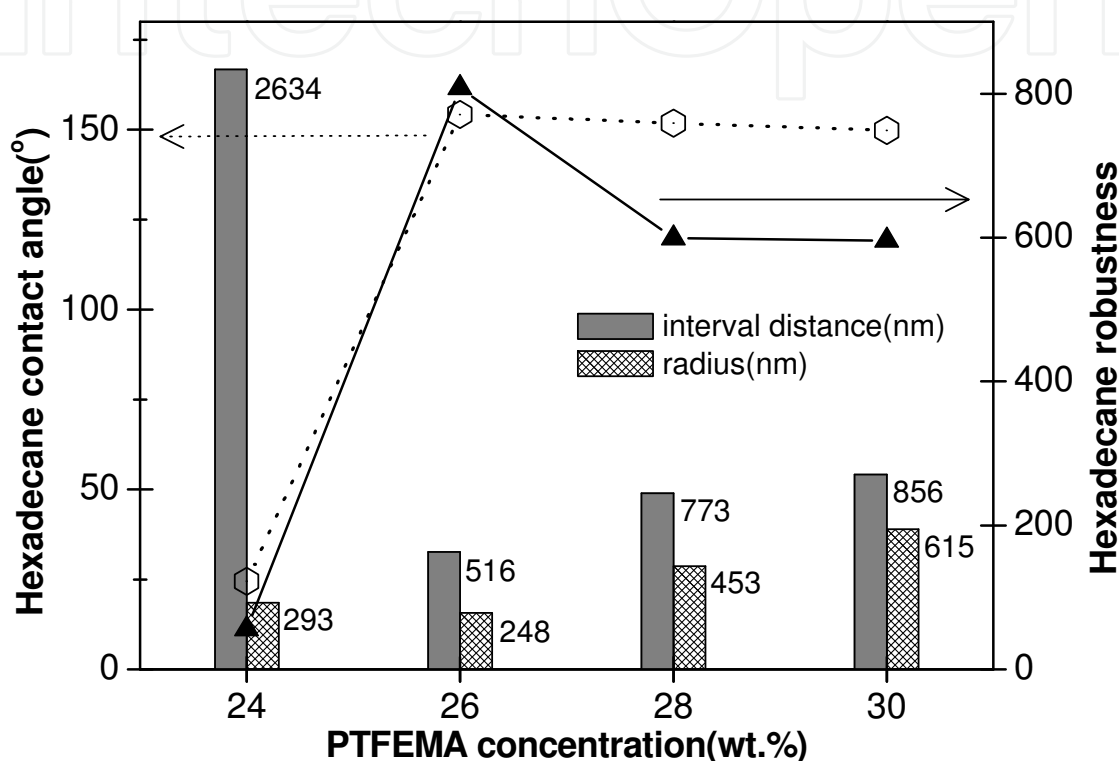
Fig. 14. The relationship between the hexadecane contact angles and the robustness with the gap distance between the fibers and the fiber radius of an electrospun web of the PTFEMA fibers with different polymer solution concentrations of 24 wt%, 26 wt%, 28 wt%, and 30 wt%. The volume of hexadecane was 6 µL in all cases [21].

3. Conclusions

Two types of nature-inspired lotus surfaces were demonstrated. A superhydrophobic and transparent biomimetic surface and a superamphiphobic electrospun nanofibers web were prepared by simple fabrication methods involving a combination of colloidal lithography and plasma etching for the former and a conventional electrospinning method with traditional processing parameters for the latter. The dual functional surfaces were introduced simply by starting with the mimicking of the lotus leaf. The simple nanostructuring process yielded a superhydrophobic structure with an antireflective property. Our study on repellence against hexadecane and water wetting reveals that a small, uniform fiber diameter and interval distance can induce a high level of robustness on a low surface tension liquid.

Beyond a Nature-inspired Lotus Surface: Simple Fabrication Approach Part I. Superhydrophobic
and Transparent Biomimetic Glass Part II. Superamphiphobic Web of Nanofibers
157

At present, many researchers are making a great effort to realize an artificial lotus leaf with advanced functions. Some of these results have moved beyond simply a lotus leaf. However, an artificial lotus leaf remains associated with problems related to its practical application. The most dissimilar aspect between nature and artificiality by humans is the ability to regenerate. We have a long way to go in this respect compared to nature. However, our attempts to live together with nature using nature-inspired technology bring sustainability and comfort to human life.

4. Acknowledgements

5. References

[1] Bhushan B. Biomimetics:Lessons from Nature – an Overview. Phil. Trans. R. Soc. A, 2009, 367: 1445-1486

[2] Neinhuis C, Barthlott W. Characterization and Distribution of Water Repellent, Self-cleaning Plant Surfaces. Ann Bot., 1977, 79: 667-677

[3] Genzer J, Efimenko K. Recent Developments in Superhydrophobic Surface and their Relevance to Marine Fouling: A Review. Biofouling, 2006, 22(5): 339-360

[4] Li X-M, Reinhoudt D, Crego-Calama M. What Do We Need for a Superhydrophobic Surface? A Review on the Recent Progress in the Preparation of Superhydrophobic Surfaces. Chem. Soc. Rev.,2007, 36: 1350-1368

[5] Martines E, Seunarine K, Morgan H, Gadegaard N, Wilkinson C D W, Riehle M O. Superhydrophobicity and Superhydrophilicity of Regular Nanopatterns. Nano Lett, 2005, 5: 2097-2103

[6] Suh K Y, Jon S. Control over Wettability of Polyethylene Glycol Surfaces using Capillary Lithography. Langmuir, 2005, 21: 6836-6841

[7] Kanamori Y. Roy E. Chen Y. Antireflection sub-wavelength gratings fabricated by spin-coating replication. Microelectron. Eng, 2005, 78-79: 287-293

[8] Gombert A, Glaubitt W, Rose K, Dreibholz J, Blasi B, Heizel A, Sporn D, Doll W, Wittwer V. Subwavelength-Structured Antireflective Surfaces on Glass. Thin Solid Films, 1999, 351: 73-77

[9] Minko S, Muller M, Motornov M, Nitschke M, Grundke K, Stamm M. Two-level Structured Self-adaptive Surfaces with Reversibly Tunable Properties. J. Am. Chem. Soc., 2003, 125: 3896-3900

[10] Noh J., Lee J.-H., Na S., Lim H., Jung D.-H. Fabrication of Hierarchically Micro- and Nano-structured Mold Surfaces Using Laser Ablation for Mass Production of Superhydrophobic Surfaces. Jpn. J. Appl. Phys., 2010, 49: 106502

[11] Ma M L, Hill R M, Lowery J L, Fridrikh S V, Rutledge G C. Elec-trospun Poly(Styrene-block-dimethylsiloxane) Block Copolymer Fibers Exhibiting Superhydrophobicity. Langmuir, 2005, 21: 5549-5554

[12] Gu G, Dang H, Zhang Z, Wu Z. Fabrication and Characterization of Transparent Superhydrophobic Thin Films based on Silica Nanoparticles. Appl. Phys. A, 2006, 83: 131-132

[13] Hosono E, Fujihara S, Honma I, Zhou H S. J. Superhydrophobic Perpendicular Nanopin Film by the Bottom-up Process. Am. Chem. Soc., 2005, 127: 13458-13459

[14] Sun T, Wang G J, Liu H, Feng L, Jiang L, Zhu D B. Suh K Y, Jon S. Control over the Wettability of an Aligned Carbon Nanotube Film. J. Am. Chem. Soc., 2003, 125: 14996-14997

[15] Zhu L B, Xiu Y H, Xu J W, Tamirisa P A, Hess D W, Wong C P. Superhydrophobicity on Two-tier Rough Surfaces Fabricated by Con-trolled Growth of Aligned Carbon Nanotube Arrays Coated with Fluorocarbon. Langmuir, 2005, 21: 11208-11212

[16] Zimmermann J., Reifler F. A., Fortunato G., Gerhardt L.-C., Seeger S. A Simple, One-Step Approach to Durable and Robust Superhydrophobic Textiles. Adv. Funct. Mater. 2008, 18: 3662-3669

[17] Lim H. S., Baek J. H., Park K., Shin H. S., Kim J., Cho J. H. Multifunctional Hybrid Fabrics with Thermally Stable Superhydrophobicity. Adv. Mater. 2010, 22, 2138-2141.

[18] Liu Y., Xiu Y., Hess D. W., Wong, C. P. Silicon Surface Structure-Controlled Oleophobicity. Langmuir, 2010, 26: 8908-8913

[19] Tuteja A., Choi W., Mabry J. M., McKinley G. H., Cohen R. E. Robust omniphobic surfaces. PNAS, 2008, 105: 18200-18205

[20] Lim H., Jung D.-H., Noh J.-H., Choi G.-R., Kim W.-D. Simple Nanofabrication of a Superhydrophobic & Transparent Biomimetic Surface. Chinese Sci. Bull., 2009, 54: 3613-3616

[21] Choi G.-R., Park J., Ha J.-W., Kim W.-D., Lim H. Superamphiphobic Web of PTFEMA Fibers via Simple Electrospinning without Functionalization. Macromol. Mater. Eng., 2010, 295:995-1002.

[22] Sun C-H, Gonzalez A, Linn N C, Jing P, Jiang B. Templated Biomi-metic Multifunctional Coatings. App. Phys. Lett., 2008, 92: 051107-051109

[23] Min W.-L., Jiang P., Jiang B. Large-Scale Assembly of Colloidal Nanoparticles and Fabrication of Periodic Subwavelength Structures. Nanotechnology 2008, 19: 475604.

[24] Quere D. Rough Ideas on Wetting. Physica A, 2002, 313: 32-37

[25] Li X.-M., Reinhoudt D., Crego-Calama M. What do we need for a superhydrophobic surface? A review on the recent progress in the preparation of superhydrophobic surfaces. Chem. Soc. Rev. 2007, 36: 1350-1368

[26] Onda T., Shibuichi S., Satoh N., Tsujii K. Super-Water-Repellent Fractal Surfaces. Langmuir, 1996, 12: 2125-2127

[27] Tuteja A., Choi W., Ma M., Mabry J. M., Mazzella S. A., Rutledge G. C., McKinley G. H., Cohen R. E. Designing Superoleophobic Surfaces. Science, 2007, 318, 1618-1622

[28] Ahuja A., Taylor J. A., Lifton V., Sidorenko A. A., Salamon T. R., Lobaton E. J., Kolodner P., Krupenkin T. N. Nanonails: A Simple Geometrical Approach to Electrically Tunable Superlyophobic Surfaces. Langmuir, 2008, 24: 9-14

[29] Leng B., Shao Z., With G., Ming W. Superoleophobic cotton textiles. Langmuir 2009, 25: 2456-2460

[30] Ramakrishna S., Fujihara K., Teo W.-E., Lim T.-C., Ma Z., An introduction electrpspinning and nanofibers, World scientific publishing Singapore 2005, Ch. 3.

[31] Ha J.-W., Park I. J., Lee S.-B., Antireflection Surfaces Prepared from Fluorinated Latex Particles. Macromolecule, 2008, 41: 8800-8806

[32] Hunley M. T., Harber A., Orlicki J. A., Rawlett A. M., Long T. E. Effect of Hyperbranched Surface-Migrating Additives on the Electrospinning Behavior of Poly(methyl methacrylate). Langmuir, 2008, 24: 654-657

Advances in Biomimetics

Edited by Prof. Marko Cavrak

The interaction between cells, tissues and biomaterial surfaces are the highlights of the book "Advances in Biomimetics". In this regard the effect of nanostructures and nanotopographies and their effect on the development of a new generation of biomaterials including advanced multifunctional scaffolds for tissue engineering are discussed. The 2 volumes contain articles that cover a wide spectrum of subject matter such as different aspects of the development of scaffolds and coatings with enhanced performance and bioactivity, including investigations of material surface-cell interactions.

How to reference

In order to correctly reference this scholarly work, feel free to copy and paste the following:

INTECH
open science | open minds